American Journal of Chemistry 2022, 12(1): 10-17
DOI: 10.5923/j.chemistry.20221201.02

# Physicochemical Characterization of Tin Oxide Synthesized from Acid Mine Drainage Using Tin II Chloride

**Alegbe M. J.[1,2,*], Moronkola BA[1], Elesho A. O.[1], Ayanda OS[3,4], Petrik L. F.[2]**

[1]Chemistry Department, Lagos State University, LASU Post office, Ojo, Lagos Badagry-expressway, Lagos, Nigeria
[2]Enviromental and NanoSciences Group, Chemistry Department, University of the Western Cape, Bellville, South Africa
[3]Department of Chemistry, Vaal University of Technology, Vanderbijlpark, South Africa
[4]Nanoscience Research, Department of Industrial Chemistry, Federal University Oye Ekiti, Oye Ekiti, Ekiti State, Nigeria

**Abstract** The chemical composition of pollutants in acid mine drainage (AMD) wastes is a great concern to the public, the mining operators and the South African government. This research is aimed at making tin oxide ($SnO_2$) from AMD. The particles were formed by chemical precipitation process which were characterized with modern analytical techniques such as X-ray diffraction (XRD), high resolution scanning electron microscopy-energy dispersing spectroscopy (HRSEM-EDS), X-ray fluorescence (XRF), high resolution transmission electron microscopy (HRTEM), Fourier transform infra-red spectroscopy (FTIR) and Brunauer-Emmett Teller (BET). The particles are formed by chemical precipitation process which was characterized with analytical techniques such as X-ray diffraction (XRD), high resolution scanning electron microscopy-energy dispersing spectroscopy (HRSEM-EDS), X-ray fluorescence (XRF), high resolution transmission electron microscopy (HRTEM), Fourier transform infra-red spectroscopy (FTIR) and Brunauer-Emmett Teller (BET). The XRD result of the precipitate identified cassiterite ($SnO_2$) mineral phase as the only crystal formed while SEM images revealed unequal size spherical in shape particles. The HRTEM revealed that the particles are crystalline with fringes and average particle size was 2 nm. In conclusion, Tin oxide nanoparticle was successfully synthesized by the chemical precipitation method from the starting material as $SnCl_2$.

**Keywords** Acid mine drainage, Tin oxide, Chemical precipitation, Characterization

## 1. Introduction

Tin oxide ($SnO_2$) is a semiconductor with optical properties and the semiconductor oxides are important for the development of smart and functional materials, devices and systems [1]. Crystalline tin oxide (cassiterite) structure is a wide band gap (3.6 eV). It is typically transparent n-type semiconductor in its grown state [2]. Semiconductor nanoparticles exhibit change in electronic properties relative to the bulk counterpart and the band gap increases as the solid becomes smaller in particle size. Semiconductor oxides have two unique structural features which are mixed cation valences and an adjustable oxygen deficiency are the basis for creating and changing several novel material properties from chemical, electrical, and optical to magnetic properties. Semiconductor oxide nanoparticles exhibit a change in the electronic properties relative to the bulk counterpart and the band gap increases as the solid becomes smaller in particle size [3]. The research on tin oxide semiconductor is experiencing rapid growth due to wide range of applications. $SnO_2$ particles are widely used in gas sensing due to their high mobility of conduction of electrons, good chemical and thermal stability under the operating condition of such as gas sensors [2] [4] [5] [7], catalyst [8] [9], photosensors [7], resistors [1], electrodes in glass melting furnaces [11], antistatic coating [12], transparent heating elements [13], batteries [14] [16] [17] [18], photocatalytic degradation of organic dyes [19] [20] [21] [22] [23], photovoltaic devices [8], high electrical conductivity with optical transparent heating elements [9], etc. The aim of this study is to use acid mine drainage (AMD) waste solution to synthesize $SnO_2$ particles using tin II chloride as the starting reagent. $SnO_2$ can be synthesized using physical method such as mechanical milling from large particle size to smaller particle sizes [24] [25] [26], and chemical methods such as chemical precipitation [27] [28] [29], hydrothermal [5] [30] [31] [32], microwave [12] [33], microwave [34], sonochemical [35], sol-gel [36] [37], solvothermal [38] [37] [39]. The size, morphology, stability and properties of

* Corresponding author:
alegbemj@gmail.com (Alegbe M. J.)
Received: Dec. 2, 2021; Accepted: Dec. 29, 2021; Published: Feb. 15, 2022
Published online at http://journal.sapub.org/chemistry

synthesized $SnO_2$ nanoparticles are of great importance and should be considered seriously [40]. Oxides of semiconductors like tin oxide have different morphologies depending on the conditions and methods of their synthesis. Their morphologies appears in different nanostructured shapes some of which are nanoflower [41] [42], nanobelt [43], nanotree [44], rods [40] [45], wires [46] [47] tubes [3], belts [43] [48], Chemical vapour deposition (CVD) process [49], needles [50] [51], nanodiskettes [52] [53], etc. Toxicity caused by $SnO_2$ nanoparticles is very low and it has no adverse health effect which means no carcinogenic effect. The cheap starting materials and other suitable parameters are very important to reduce cost of synthesizing $SnO_2$ nanoparticles. Therefore, it is very important to design a method of synthesis using cheap and non-toxic reagents.

## 2. Materials and Methods

### 2.1. Chemical and Reagents

Raw mine water was collected from Navigation core mining site in Mpumalanga, South Africa was collected in 5L plastic containers and stored in the refrigerator regulated at a temperature of 4℃. The AMD sample was filtered with 0.45 µm membrane filter in order to remove particulate materials present in the mine solution. All chemicals used include absolute alcohol (99.5%) and tin II chloride were reagent grade chemicals purchased from Merck chemicals and used without further treatment or purification.

### 2.2. Chemical Precipitation

Different concentrations (0.1 M, 0.2 M, 0.3 M, 0.4 M, and 0.5 M) of tin II chloride solution were prepared in five different 250 mL beakers each. A volume of 50 mL of tin II chloride solution was measured into 100 mL acid mine (AMD) solution as received from the mine. The solution mixture was subjected to constant continuous vigorous agitation with a magnetic stirrer at 250 rpm for 60 minutes contact time. Yellow precipitate was formed as the tin II chloride solution was gradually added to the acidic mine solution and the precipitate was filtered and washed with 100 mL of distilled water thrice and dried in a regulated oven at a temperature of 104℃ for a period of 3 hours. The weight of the residue was recorded and the drying process continued until a constant weight was obtained. The effect of contact time was investigated by measuring 50 mL of 0.04 M of tin II chloride and added drop wise into 100 mL of raw AMD solution at different contact time of 30, 60 90, 120 and 150 minutes. The same process of rinsing, drying and weighing was carried out for the precipitate formed.

$$2SnO\,(H_2O)\,(s) \longrightarrow 2SnO_2\,(s) + 2H_2\,(g) \quad (1)$$

### 2.3. Characterization

The precipitate was characterized by using analytical techniques such as X-ray diffraction (XRD). The precipitate was identified with an X-ray powder diffraction patterns using a Bruker D8 Advance X-ray diffractometer with Cu Kα radiation (λ = 1.542 Å) with operating current and voltage of 40 mA and 40 kV respectively. The precipitate was scanned at the rate of 0.02° (10 s per step) at diffraction angle 2θ range from 20-80°. The morphology and particle size of precipitate was examined with both high resolution and high resolution scanning electron microscopy (HRSEM). The scanning electron microscopy energy dispersive spectroscopy (SEM-EDS) technique was used to provide available information on morphology and surface texture of individual particle as well as the chemical composition of the elements present in the precipitate. For the SEM analysis, a small quantity of sample was put on carbon coated sample holder stub with a gentle blow applied to remove loosely bound particles and the remaining dust particles were stuck to the carbon coat on the sample holder to dry at room temperature before it was examined under the SEM measurement using a HITACHI S-4700 electron microscope. The precipitate was dried and used for morphological analysis using Phillips Tecnai F20 super-twain HRTEM. Little amount of the precipitate was placed in sample bottle containing 5 mL absolute alcohol and sonicated for 10 minutes to obtain a good particle dispersal on the copper grid and allowed to dry at room temperature. The analysis was carried out to examine the size and morphology of the precipitate. Fourier transform infrared (FTIR) spectroscopy was conducted to identify the functional groups present in the precipitate. The FTIR analysis was conducted with Perkin Elmer RX1 series FTIR spectrometer to record the IR spectra of the sample. The analysis is for phase purity, and to identify related functional group in the precipitate. Small amount of the precipitate was required for the functional group analysis. The sample was mixed with KBr at different ratios to make it in pellets form and dried in a regulated oven at 105℃ for 12 hours to remove any trace of moisture present in the precipitate. Brunauer-Emmette-Teller (BET) surface area of the precipitate was measured at a temperature of 77.35K using nitrogen adsorption method with a quantachrome NOVA 2000 surface analyzer. The surface area of the sample was prepared by washing the precipitate with acetone and dried at 100℃ for 5-8 hours under constant flow of nitrogen gas. The sample powder was dried in an oven regulated at 105℃ for 12 hours to remove any trace of moisture present in the sample.

## 3. Results

The optimization of tin II chloride concentration and contact time of synthesizing $SnO_2$ is presented in Figures 1 and 2. The optimized concentration of tin II chloride and contact time in Figures 1 and 2 are 0.04 M and 60 minutes respectively. The optimum concentration yielded a mass of 0.79 g while the contact time was 0.64 g.

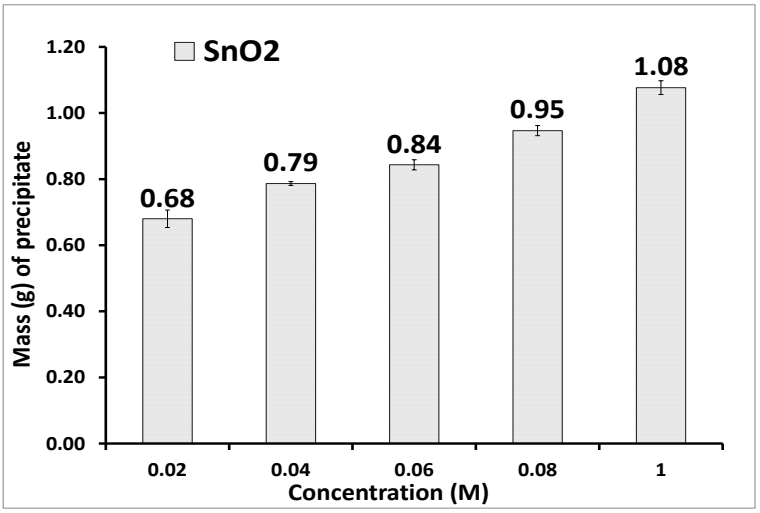


**Figure 1.** Concentration (M) of tin II chloride. Experimental conditions: pH of AMD = 2.14, vol. of AMD = 100 mL, vol. of $SnCl_2$ = 50 mL, contact time = 60 minutes, n = 3

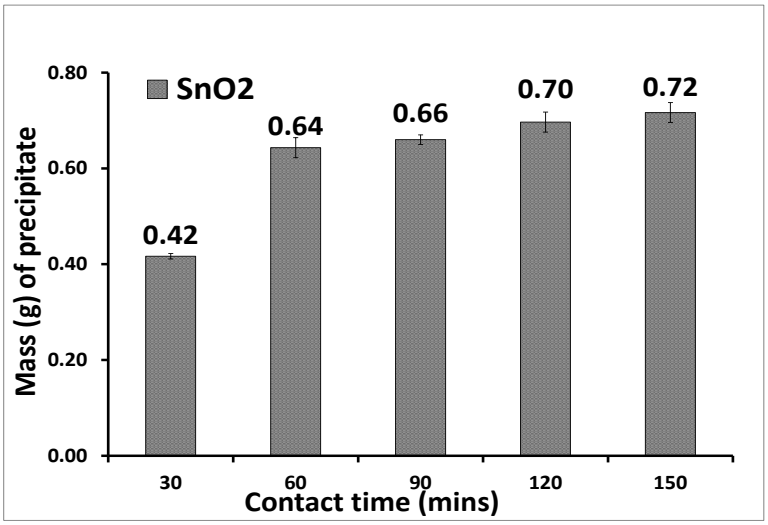


**Figure 2.** Contact time of precipitating tin oxide. Experimental conditions: pH of AMD = 2.14, vol. of AMD = 100 mL, vol. of $SnCl_2$ = 50 mL, optimum concentration = 0.04 M, n = 3

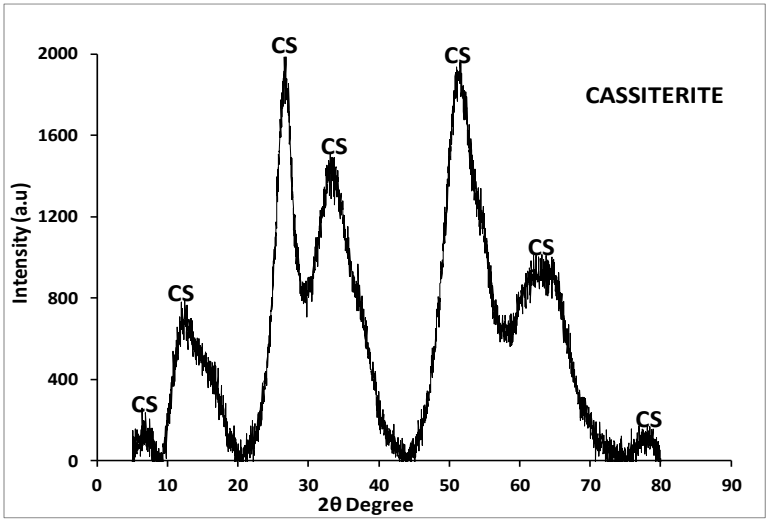


**Figure 3.** Powder X-Ray diffraction pattern of Cassiterite ($SnO_2$) synthesized from the AMD: Experimental conditions: pH of AMD = 2.14, vol. of AMD = 100 mL, conc. of $SnCl_2$ = 0.04 M, vol. of $SnCl_2$ = 50 mL, contact time = 60 minutes, n = 3, CS = cassiterite ($SnO_2$)

The precipitate was taken for analyzes so as to assess its quality. Figure 3 presents the result of the XRD diffraction pattern of the precipitates formed from the treatment of AMD with tin II chloride reductant. The mineral phase identified was tin oxide or cassiterite ($SnO_2$). The diffraction pattern of the crystallite appears at reflection angle 2θ indexed at 27°, 3[°] 51° and 65° which correspond to (110), (101), (211) and (301) lattice plane base on tetragonal phase of cassiterite ($SnO_2$) (JCPDS File No. 41-1445, a = b = 4.738 Å, and c = 3.178 Å) were indexed to cassiterite ($SnO_2$) structure. No other characteristic diffraction peaks due to metallic tin (Sn) or tin oxides was observed therefore, the crystal was purely cassiterite ($SnO_2$). Park et al. [2] reported that similar result was obtained in the synthesis of SnO2. The polycrystalline diffraction of cassiterite ($SnO_2$) was revealed by the first three predominant peaks exhibited at (110), (101) and (211) planes. The same peaks of the crystallite was also observed to be broad which can be attributed to the small size of the particles [54]. The broadening of the XRD peaks revealed the characteristic of cassiterite ($SnO_2$). The result obtained from the XRD analysis of cassiterite crystallite agrees with that obtained in the literature [54] [55] [56] [57] [58] [59].

The average crystalline size of the tin oxide nanoparticle were calculated using Debye Scherrer formula, $D = K\lambda / \beta Cos\theta$

Where D is the mean crystalline size, K is a grain shape dependent constant (0.9), λ is the wavelength of the incident beam, θ is a Bragg reflection angle and β is the full width half maximum.

**Table 1.** Energy dispersive spectroscopy (EDS) chemical composition of Cassiterite ($SnO_2$) synthesized from AMD. Experimental conditions: pH of AMD = 2.14, vol. of AMD = 100 mL, conc. of $SnCl_2$ = 0.04 M, vol. of $SnCl_2$ = 50 mL, contact time = 60 minutes, n = 3, $SnCl_2$

| Element | % Atm. Wt | Stdev |
|---|---|---|
| **Sn** | 65.5 | 5.73 |
| **O** | 31.96 | 1.25 |
| **Cl** | 2.54 | 0.97 |

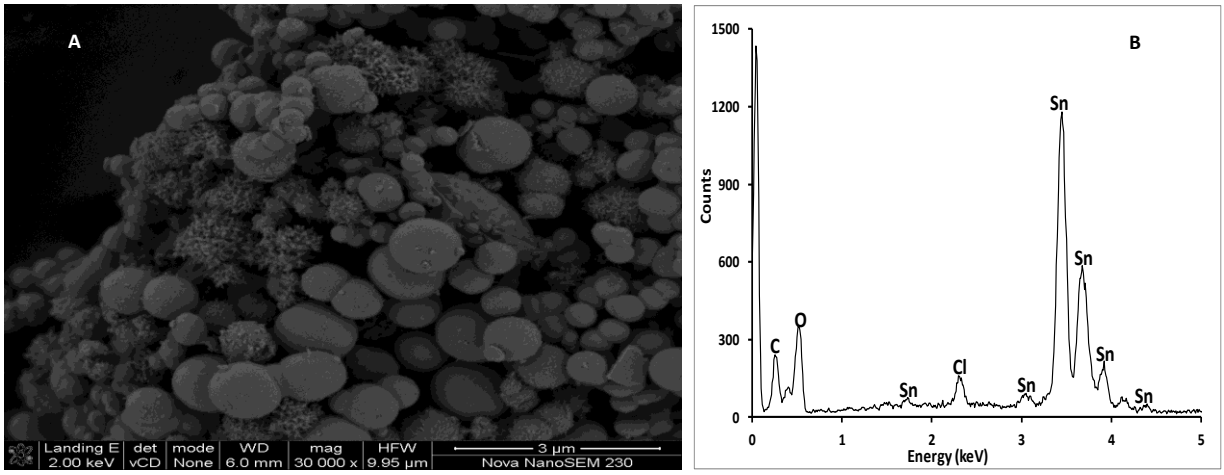


**Figure 4.** SEM morphology (A) and EDS spectrum (B) of cassiterite ($SnO_2$) synthesized from AMD. Experimental conditions: pH of AMD = 2.14, vol. of AMD = 100 mL, conc. of $SnCl_2$ = 0.04 M, vol. of $SnCl_2$ = 50 mL, contact time = 60 minutes, n = 3

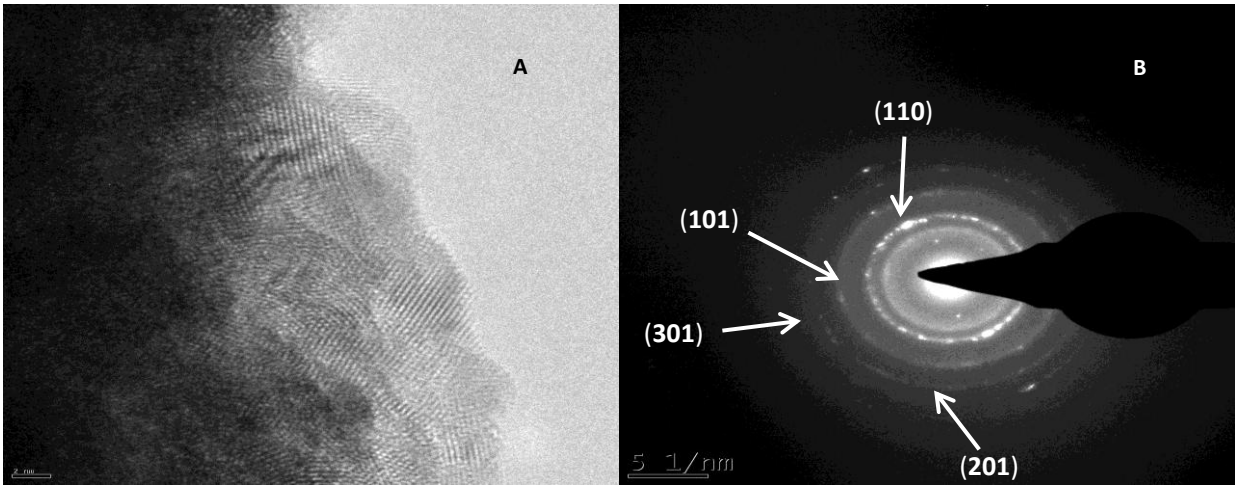


**Figure 5.** HRTEM morphology (A), SAED, (B) of cassiterite ($SnO_2$) synthesized from AMD. Experimental conditions: pH of AMD = 2.14, vol. of AMD = 100 mL, conc. of $SnCl_2$ = 0.04 M, vol. of $SnCl_2$ = 50 mL, contact time = 60 minutes, n = 3

Figure 4 presents the SEM morphology (A) and the EDS spectrum (B) of the elements found in the crystals synthesized from the reaction mixture of AMD collected from Navigation coal mine with $SnCl_2$ as reductant. The surface morphology of the residues is spherical in shape with different sizes and there are some irregular crystals around the spheres. The EDS spectrum revealed that the chemical composition of the cassiterite are Sn, O and Cl. Table 1 presents the EDS of cassiterite ($SnO_2$) synthesized from the treatment of AMD with tin II chloride solution. The EDS revealed that the chemical composition of the particles was made up of 65.5% of Sn, 31.96% of O, and 2.54% of Cl. The product is composed mainly of tin and the presence of carbon is from the sample stub. The trace of chlorine detected (2.54%) comes from the tin II chloride used in the precipitation process as presented in Table 1. The composition of the elements present in the synthesized sample confirmed that the mineral phase of the sample was cassiterite ($SnO_2$).

Figure 5 presents the HRTEM micrograph of $SnO_2$ nanoparticle (A), selected area electron diffraction [SAED] (B) results of $SnO_2$ crystallite formed from the treatment of AMD with tin II chloride as reductant. The morphology of the $SnO_2$ showed high resolution fringes which indicate that the crystallite was crystalline with an average crystal size range from 1.5 - 2 nm as measured with imageJ software. The selected area electron diffraction ring showed tiny spots round the ring which indicates that it is polycrystalline. The lattice fringes spacing of $SnO_2$ nanoparticles shows contribution mainly from (110) and (101) planes. The selected area electron diffraction ring showed tiny spots round the ring which indicates that it is polycrystalline. The lattice fringe spacing of $SnO_2$ nanoparticles shows contribution mainly from (110) and (101) planes. The selected area electron diffraction ring showed tiny spots round the ring which indicates that it is polycrystalline. Fast Fourier transform (FFT) analysis of selected regions of the coating reveals details of the local $SnO_2$ structure. The corresponding ring pattern of SAED (B) confirmed the presence of single crystalline cassiterite ($SnO_2$) phase nanoparticles. It reveals the presence of fluffy particles that looks like agglomerated tin oxide nanoparticle with uniform particle size ranging from 2 to 3 nm which confirms the presence of single-crystal $SnO_2$ nanostructure.

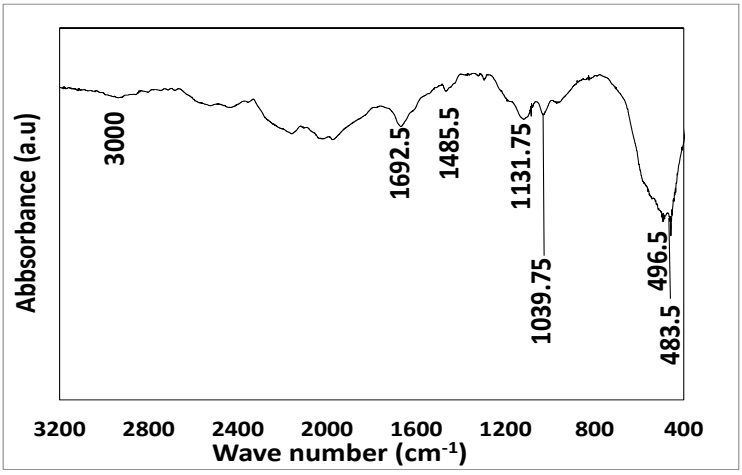


**Figure 6.** FTIR absorption spectrum of cassiterite synthesized from AMD. Experimental conditions: pH of AMD = 2.14, vol. of AMD = 100 mL, conc. of $SnCl_2$ = 0.04 M, vol. of $SnCl_2$ = 50 mL, contact time = 60 minutes, n = 3

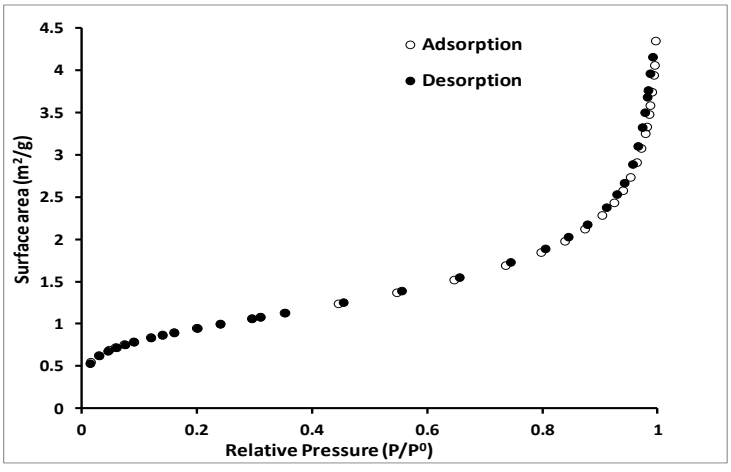


**Figure 7.** Nitrogen adsorption-desorption isotherm of cassiterite ($SnO_2$) synthesized from AMD. Experimental conditions: pH of AMD = 2.14, vol. of AMD = 100 mL, conc. of $SnCl_2$ = 0.04 M, vol. of $SnCl_2$ = 50 mL, contact time = 60 minutes, n = 3

Figure 6 presents the FTIR absorption spectrum of cassiterite obtained from reaction of AMD with tin II chloride solution. Fourier transform infrared (FTIR) analysis of selected regions of the coating reveals the details of the local $SnO_2$ structure. The cassiterite crystal showed absorption peaks at 483.5 $cm^{-1}$, 496.5 $cm^{-1}$, 1039.75 $cm^{-1}$, 1131.75 $cm^{-1}$, 1485.5 $cm^{-1}$, 1692.5 $cm^{-1}$ and 3000 $cm^{-1}$. The Sn-O bond exhibits its stretching vibration mode at absorption band of 464 $cm^{-1}$ and 503.3 $cm^{-1}$. The absorption band at 483.3 $cm^{-1}$ and 503.3 $cm^{-1}$ in the FTIR spectrum can be assigned to lattice vibration stretching mode of Sn-O and OSnO respectively. Studies have shown that SnO and OSnO absorption bands at 400-800 $cm^{-1}$ are characteristic of nanocrystalline cassiterite structure which contain bound OH group [60]. The broad water absorption band with OH group vibration stretching was observed at 2800-3450 $cm^{-1}$ and the bending vibration of water OH group at 1643-1665 $cm^{-1}$. The absorption band at 1031 $cm^{-1}$ and 1117.3 $cm^{-1}$ resemble those assigned to Sn-OH modes [61]. The result obtained in this study is within the range attributed to tin oxide in the literature [40] [61] [62] [63]. The SnO particle is metastable and will decompose to $SnO_2$ and $H_2$ when subjected to drying or evaporation at a high temperature above 100-150℃.

The SnO particle is metastable and will decompose to $SnO_2$ and $H_2$ when subjected to drying or evaporation at a high temperature above 100-150℃. The SnO particle is metastable and will decompose to $SnO_2$ and $H_2$ when subjected to drying or evaporation at a high temperature above 100-150℃. The SnO particle is metastable and will decompose to $SnO_2$ and $H_2$ when subjected to drying or evaporation at a high temperature above 100-150℃. BET surface area of cassiterite from the treatment of AMD with tin II chloride is presented in Figure 7.

Figure 7 presents the nitrogen adsorption-desorption isotherm of cassiterite ($SnO_2$) synthesized from the reaction between AMD and tin II chloride salt solution. The hysteresis loop of the $SnO_2$ sample adsorption classification was Type II and the adsorption-desorption classification was H3 and the BET surface area obtained for the $SnO_2$ particle was 7.7 $m^2/g$. The BET surface area obtained in this study was very low compared to 35 $m^2/g$ reported in the literature for the reagent grade synthesized cassiterite [56] [57] [58] [64].

## ACKNOWLEDGMENTS

This research was supported in part by the Water Research Commission, South Africa and technical support was provided by contributions to this research work: Water Research Commission (WRC) South Africa, Dr. Remy Bucker National Research Fund (NRF) Ithemba-labs, Western Cape, South Africa, Mrs. Ilse Wells, University of The Western Cape (UWC), South Africa and Mrs. Miranda Waldron, University of Cape Town (UCT), South Africa, and Dr. Avoseh Opeyemi, Lagos State University.

## REFERENCES

[1] Wang ZL (2003). Nanobelts, Nanowires, and Nanodiskettes of Semiconducting oxides: Adv Mater, 15, No 5, 423-436.

[2] Park MS., Wang GX., Kang YM., Wexler D., Dou SX., Liu HK (2007). Preparation and Electrochemical Properties of SnO2 Nanowires for Application in Lithium-Ion Batteries, Angew. Chem. Int. Ed. 2007, 46, 750 –753.

[3] Shi L., Lin H (2011). Preparation of Band Gap Tunable SnO2 Nanotubes and Their Ethanol Sensing Properties. Langmuir, 2011, 27, 7, 3977-3981.

[4] Han X., Jin M., Xie S., Kuang Q., Jiang Z., Jiang Y., Xie Z., Zheng L (2009). Synthesis of Tin Dioxide Octahedral Nanoparticles with Exposed High-Energy {221} Facets and Enhanced Gas Sensing Properties. Angew. Chem. Int. Ed 2009, vol. 48, pp. 9180-9183.

[5] Matin BM., Mortazavi Y., Khodadadi AA., Abbasi A., Firooz AA (2010). Alkaline- and template-free hydrothermal synthesis of stable SnO2 nanoparticles and nanorods for CO and ethanol gas sensing. Sensors and Actuators B: Chemical, Volume 151, Issue 1, 26 November 2010, Pages 140-145.

[6] Cukrov LM., McCormick PG., Galatsis K., Wlodarski W (2007). Gas sensing properties of nanosized tin oxide synthesized by mechanochemical processing, Sens. Actuators B 77 491-495. (Author links open overlay panel L.M. Cukrov, P.G. McCormick, K Galatsis, W. Wlodarski).

[7] Pandey PC., Upadhyay BC., Pandey CMD., Pathak HC (1999). Electrochemical studies on D96N bacterior hodopsin and its application in the development of photosensors, Sensors and Actuators B: Chemical, 56 112-120.

[8] Hong ZR., Liang CJ., Sun XY., Zeng XT (2006). Characterization of organic photovoltaic devices with indium-tin-oxide anode treated by plasma in various gases, J. Appl. Phys. 100 (2006) 093711. (ZR Hong, CJ Liang, XY Sun, XT Zeng - Journal of applied physics, 2006 - aip.scitation.org).

[9] Batzill M, Diebold U, (2005). The surface and materials science of tin oxide. Progress in Surface Science 79 (2005) 47–154.

[10] Pinna N., Neri G., Antonietti M., Niederberger M (2004). Nonaqueous Synthesis of Nanocrystalline Semiconducting Metal Oxides for Gas Sensing. A journal of German chemical society, pp 235-240. (Nicola Pinna, Giovanni Neri, Markus Antonietti, Markus Niederberger).

[11] Fourcade, J., & Citti, O. (2013). New Tin Oxide Electrodes for Glass Melting. In 73rd Conference on Glass Problems (pp. 183-199). Hoboken, NJ, USA: John Wiley & Sons, Inc.

[12] Krishnakumar T., Pinna N., Prasanna K., Kumari K., Perumal K., Jayaprakash R (2008). Microwave assisted synthesis and characterization of tin oxide nanoparticles, Mater. Lett. 62 3437-3440.

[13] Moon, H. G., Shim, Y. S., Jeong, H. Y., Jeong, M., Jung, J. Y., Han, S. M., ... & Jang, H. W. (2012). Self-activated ultrahigh chemosensitivity of oxide thin film nanostructures for transparent sensors. Scientific reports, 2(1), 1-7.

[14] Branci C., Benjelloun N., Sarradin J., Ribes M (2000). Vitreous tin oxide-based thin film electrodes for Li-ion micro-batteries, Solid State Ionics, 135 169-174.

[15] Chen Y., Kanan MW (2012). Tin Oxide Dependence of the CO2 Reduction Efficiency on Tin Electrodes and Enhanced Activity for Tin/Tin Oxide Thin-Film Catalysts. Journal of the American Chemical Society.

[16] Vijayaraghavan SN., Wall J., Li L., Xing G., Zhang Q., Yan F. 2020. Low-temperature processed highly efficient hole transport layer free carbon-based planar perovskite solar cells with SnO2 quantum dot electron transport layer. Materials Today Physics, 13, 100204. https://doi.org/10.1016/j.mtphys.2020.100204.

[17] Shang G., Wu J., Huang M., Lin J., Lan Z., Huang Y., Fan L (2012). Facile Synthesis of Mesoporous Tin Oxide Spheres and Their Applications in Dye-Sensitized Solar Cells. J. Phys. Chem. C, 116, 38, 20140.

[18] Belliard, F., Connor, P. A., & Irvine, J. T. S. (2000). Novel tin oxide-based anodes for Li-ion batteries. Solid state ionics, 135(1-4), 163-167.

[19] Sani KI, Gaya U, Hamisu A (2021). Synthesis of Visible Light Response S-SnO2 Catalyst for Optimized Photodegradation of Bromophenol Blue. Journal of Physical Chemistry and Functional Materials, https://doi.org/10.54565/jphcfum.1008388.

[20] Suresh KC, Surendhiran S, Kumar PM, Kumar ER, Khadar YAS, Balamurugan A (2020). Green synthesis of SnO2 nanoparticles using Delonix elata leaf extract: Evaluation of its structural, optical, morphological and photocatalytic properties. SN Applied Sciences, 2 (10) https://doi.org/10.1007/s42452-020-03534-z.

[21] Elango G., Roopan SM (2016). Efficacy of SnO2 nanoparticles toward photocatalytic degradation of methylene blue dye. Journal of Photochemistry and Photobiology B: Biology, Volume 155, February 2016, Pages 34-38.

[22] Yuvakkumar, R., Elango, V., Rajendran, V., & Kannan, N. (2011). Preparation and characterization of zero valent iron nanoparticles. Digest Journal of Nanomaterials and Biostructures, 6(4), 1771--1776.

[23] Kansala SK., Singh M., Sud D (2007). Studies on photodegradation of two commercial dyes in aqueous phase using different photocatalysts. Journal of Hazardous Materials. Volume 141, Issue 3, 22, Pages 581-590.

[24] Cho, H., Waters, M. A., & Hogg, R. (1996). Investigation of the grind limit in stirred-media milling. International Journal of Mineral Processing, 44, 607-615.

[25] Knieke, C., Sommer, M., & Peukert, W. (2009). Identifying the apparent and true grinding limit. Powder Technology, 195(1), 25-30.

[26] Stenger, F., Mende, S., Schwedes, J., & Peukert, W. (2005). Nanomilling in stirred media mills. Chemical Engineering Science, 60(16), 4557-4565.

[27] Yu D., Wang D., Yu W., Qian Y (2006). Synthesis of ITO nanowires and nanorods with corundum structure by a co-precipitation method, Mater. Lett. 58 (2006) 84-87.

[28] Song KC., Kang Y (2000). Preparation of high surface area tin oxide powders by a homogeneous precipitation method. Materials Letters, Volume 42, Issue 5, Pages 283-289.

[29] Tazikeh S., Akbari A., Talebi A., TaleB, E (2014). Synthesis and characterization of tin oxide nanoparticles via the Co-precipitation method. Materials Science-Poland, 32(1), 2014, pp. 98-101.

[30] Li Z., Li X., Zhang X., Qian Y (2006). Hydrothermal synthesis and characterization of novel flower-like zinc doped SnO2 nanocrystals, J. Crystal Growth, 291 258-261.

[31] Tan L., Wang L., Wang Y (2011). Hydrothermal Synthesis of SnO2 Nanostructures with Different Morphologies and Their Optical Properties. Journal of Nanomaterials, Volume 2011, Article ID 529874, pages 1-10. doi:10.1155/2011/529874.

[32] Talebian N., Jafarinezhad F (2013). Morphology-controlled synthesis of SnO2 nanostructures using hydrothermal method and their photocatalytic applications. Ceramics International, Volume 39, Issue 7, September 2013, Pages 8311-8317.

[33] Motshekga SC., Pillai SK., Ray SS., Jalama K., Krause RWM (2012). Recent Trends in the Microwave-Assisted Synthesis of Metal Oxide Nanoparticles Supported on Carbon Nanotubes and Their Applications Journal of Nanomaterials, Volume 2012, Article ID 691503, 15 pgs 1-15. doi:10.1155/2012/691503.

[34] Pires FI., Joanni E., Savu R., Zaghet MA., Longo E., Varela JA (2008). Microwave-assisted hydrothermal synthesis of nanocrystalline SnO powders. Materials Letters, 62, 239-242.

[35] Hu XL., Zhu YJ., Wang SW (2004). Sonochemical and microwave assisted synthesis of linked single crystalline ZnO rods, Mater. Chem. and Phys. 88 421-426.

[36] Shek CH., Lai JKL., Lin GM (1999). Grain growth in nanocrystalline SnO2 prepared by sol-gel route, Nanostrut. Mater. 11 887-893.

[37] Gu F., Wang SF., Lu MK., Zhou GJ., Xu D., Yuan DR (2004). Photoluminescence Properties of SnO2 Nanoparticles Synthesized by Sol-Gel Method. J. Phys. Chm., vol 108, 24, 8119-7123. (Feng Gu, Shu Fen Wang, Meng Kai Lü, Guang Jun Zhou, Dong Xu Duo, Rong Yuan).

[38] Ahmad T., Khatoon S., Coolahan K (2016). Structural, Optical, and Magnetic Properties of Nickel-Doped Tin Dioxide Nanoparticles Synthesized by Solvothermal Method. Journal of the American Ceramic Society, Volume 99, Issue 4, April 2016.

[39] Han Z., Guo N., Li F., Zhang W., Zhao H., Qian Y (2001). Solvothermal preparation and morphological evolution of stannous oxide powders, Mater. Lett. 48 99-103.

[40] Wang Y., Lee JY (2004). Molten salt synthesis of tin oxide nanorods: morphological and electrochemical features. The Journal of Physical Chemistry B, 108 (46), 17832-17837. Aspects, 259(1), 151-154.

[41] Chen A., Peng X., Koczkur K., Miller B (2004). Super-hydrophobic tin oxide nanoflowers. Chem. Commun., 1964-1965. DOI: 10.1039/B407313D.

[42] A. Firooz A., Mahjoub AR., Khodadadi AA (2009). Effects of flower-like, sheetlike and granular SnO2 nanostructures prepared by solid-state reactions on CO sensing, Mater. Chem. Phys. 115 196–199.

[43] Kolmakov A., Klenov DO., Lilach Y., Stemmer S.,

Moskovits M (2005). Enhanced Gas Sensing by Individual SnO2 Nanowires and Nanobelts Functionalized with Pd Catalyst Particles. Nano Lett. 2005, 5, 667 – 673.

[44] Dick KA., Deppert K., Larsson MW., Martensson T., Seifert W., Wallenberg LR., Samuelson (2004). Synthesis of branched 'nanotrees' by controlled seeding of multiple branching events. Nat. Mater. 3, 380–384.

[45] Han X., Jin M., Xie S., Kuang Q., Jiang Z., Jiang Y., Xie Z., Zheng L (2009). Synthesis of Tin Dioxide Octahedral Nanoparticles with Exposed High-Energy {221} Facets and Enhanced Gas Sensing Properties. Angew. Chem. Int. Ed 2009, vol. 48, pp. 9180-9183.

[46] Hrkac V., Wolff N., Duppel V., Paulowicz I., Adelung R., Mishra YK., Kienle L (2019). Atomic structure and crystallography of joints in SnO2 nanowire networks. Applied Microscopy, 2019, 49:1.

[47] Zou Y., Zhang Y., Hu Y., Gu H (2018). Ultraviolet Detectors Based on Wide Band gap Semiconductor Nanowire: A Review. Sensors, 18, 1-25, 2072; doi:10.3390/s18072072.

[48] Pan ZW., Dai ZR., Wang ZL., Geim A., Novoselov K., Dimitrakopoulos C (2001). Nanobelts of Semiconducting Oxides. Science 09 Mar 2001: Vol. 291, Issue 5510, pp. 1947-1949. DOI: 10.1126/science.1058120.

[49] Mathur S., Barth H., Pyun JC., Werner U (2005). Size-Dependent Photoconductance in SnO2 Nanowires. Small, Volume1, Issue7, July 2005, Pages 713-717.

[50] Kim HW., Shim SH (2006). Synthesis and characteristics of SnO2 needle-shaped nanostructures. Journal of Alloys and Compounds, 426, 286–289 Journal of the American Ceramic Society.

[51] Yogamalar R., Mahendran V., Srinivasan R., Beitollahi A., Kumar RP., Bose AC., Vinu A (2010). Gas-Sensing Properties of Needle-Shaped Ni-Doped SnO2 Nanocrystals Prepared by a Simple Sol–Gel Chemical Precipitation Method. Chemistry an Asian Journal, vol 5, 11, pp. 2379-2385.

[52] Dai ZR., Pan ZW., Wang ZL (2002). Growth and Structure Evolution of Novel Tin Oxide Diskettes. J. Am. Chem. Soc. 2002124298673-8680.

[53] Dai ZR., Pan ZW., Wang ZL (2003). Novel Nanostructures of Functional Oxides Synthesized by Thermal Evaporation. Advanced Functional Materials, vol. 13, 1, pp. 9-24 (nanodiskette.

[54] Jiang L., Sun G., Zhou Z., Sun S., Wang Q., Yan S., Li H., Tian J., Guo J., Zhou B., Xin, Q (2005). Size-Controllable synthesis of monodispersed SnO2 nanoparticles and application in electrocatalysts. J. Phys. Chem. B, 109, 8774-8778.

[55] Kundu VS., Dhiman R., Singh D., Maan A., Arora S (2013). Synthesis and Characterization of Tin Oxide Nanoparticles via Sol-Gel Method Using Ethanol as Solvent. International Journal of Advance Research in Science and Engineering IJARSE, 2(1), 1-5.

[56] Lim HN., Nurzulaikha R., Harrison I., Lim SS., Tan WT., Yeo MC (2011). Spherical Tin Oxide, SnO2 Particles Fabricated via Facile Hydrothermal Method for Detection of Mercury (II) Ions. Int. J. Electrochem. Sci., 6, 4329-4340.

[57] Mendes PG., Moreira ML., Tebcherani SM., Orlandi MO., Andrés J., Li MS., Diaz-Mora N., Varela JA., Longo E (2012). SnO2 nanocrystals synthesized by microwave-assisted hydrothermal method: towards a relationship between structural and optical properties. Journal of Nanoparticle Research, 14(3), 1-13.

[58] Zhang X., Lin Y., Shan X., Chen Z (2010). Degradation of 2, 4, 6-trinitrotoluene (TNT) from explosive wastewater using nanoscale zero-valent iron. Chemical engineering Journal, 158(3), 566-570. (Author links open overlay panel Xin Zhang, Yu-man Lin, Xaio-quan Shan, Zu-liang Chen).

[59] Zhao H., Holladay JE., Brown H., Zhang ZC (2007). Metal chlorides in ionic liquid solvents convert sugars to 5-hydroxymethylfurfural. Science, 316(5831), 1597-1600.

[60] Gavrilenko O., Pashkova E., Belous A (2007). Effect of synthesis methods on the morphology of nanosized tin dioxide particles. Russian Journal of Inorganic Chemistry, 52(12), 1835-1839.

[61] de Monredon S., Cellot A., Ribot F., Sanchez C., Armelao L., Gueneau L., Delattre L (2002). Synthesis and characterization of crystalline tin oxide nanoparticles. J. Mater. Chem., 12, 2396–2400.

[62] Deng H., Lamelas F., Hossenlopp JM (2003). Synthesis of tin oxide nanocrystalline phases via use of tin (II) halide precursors. Chemistry of materials, 15(12), 2429-2436.

[63] Wang Y., Ma C., Sun X., Li H (2002). Preparation and characterization of SnO2 nanoparticles with a surfactant-mediated method. Nanotechnology, 13, 565-569. (Yu-de Wang, Chun-lai Ma, Xiao-dan Sun and Heng-de Li).

[64] Jouhannaud J., Rossignol J., Stuerga D (2008). Rapid synthesis of tin (IV) oxide nanoparticles by microwave induced thermohydrolysis. Journal of Solid State Chemistry, 181(6), 1439-1444.